

# The Worrisome Impact of an Inter-rater Bias on Neural Network Training

Or Schwartzman<sup>1,2</sup>, Harel Gazit<sup>1,2</sup>, Ilan Shelef<sup>2,3,4</sup>, and Tammy Riklin-Raviv<sup>1,2</sup>

<sup>1</sup> Electrical and Computer Engineering Department, Ben-Gurion University

<sup>2</sup> The Zlotowski Center for Neuroscience, Ben-Gurion University

<sup>3</sup> Department of Radiology, Soroka Medical Center

<sup>4</sup> Department of Health Sciences, Ben-Gurion University

**Abstract.** The problem of inter-rater variability is often discussed in the context of manual labeling of medical images. It is assumed to be bypassed by automatic **model-based** image segmentation approaches, which are considered ‘objective’, providing single, deterministic solutions. However, the emergence of data-driven approaches such as Deep Neural Networks (DNNs) and their application to supervised semantic segmentation - brought this issue of raters’ disagreement back to the front-stage.

In this paper, we highlight the issue of inter-rater bias as opposed to random inter-observer variability and demonstrate its influence on DNN training, leading to different segmentation results for the same input images. In fact, lower overlap scores (e.g. DICE scores) are obtained between the outputs of a DNN trained on annotations of one rater and tested on another. Moreover, we demonstrate that inter-rater bias in the training examples is amplified and become more consistent when considering the segmentation predictions of the DNNs’ test data. We support our findings by showing that a classifier-DNN trained to distinguish between raters based on their manual annotations performs better when the automatic segmentation predictions rather than the actual raters’ annotations were tested.

For this study, we used two different datasets: the ISBI 2015 Multiple Sclerosis (MS) challenge dataset, which includes MRI scans each with annotations provided by two raters with different levels of expertise [2]; and Intracerebral Hemorrhage (ICH) CT scans with manual and semi-manual segmentations [8]. The results obtained allow us to underline a worrisome clinical implication of a *DNN bias induced by an inter-rater bias* during training. Specifically, we present a consistent underestimate of MS-lesion loads when calculated from segmentation predictions of a DNN trained on input provided by the less experienced rater. In the same manner, the differences in ICH volumes calculated based on outputs of identical DNNs, each trained on annotations from a different source are more consistent and larger than the differences in volumes between the manual and semi-manual annotations used for training.

## 1 Introduction

Semantic image segmentation plays an essential role in biomedical imaging analysis. It is considered a challenging task not necessarily due to moderate image quality but mainly since it is not well defined. Different human raters and even the same rater at different time points may draw the boundary of a particular region of interest (ROI) in different manners, see e.g., [7, 9]. To address this well-known issue, an Expectation Maximization (EM) framework has been suggested for simultaneous evaluation of the raters' performance level and the consensus segmentation [17]. In [6] the variability of experts annotations was discussed in the context of segmentation evaluation. Standardizing measures to assess human observer variability for clinical studies was suggested in [13].

Machine vision algorithms are often praised for being repeatable and objective. This is, however, true only when considering deterministic, model-based approaches and obviously, the resulting segmentation is model-dependent. The emergence of machine learning and deep learning, in particular, have made data-driven approaches dominant. A supervised deep neural network (DNN) for image segmentation is trained by input images and their corresponding manual annotations that are used for calculating the network's loss. Backpropagation guided by the loss enables implicit modeling, learned indirectly from the conditional distribution of the data. This process has shown to be very powerful, outperforming model-based segmentation approaches, as it allows us to generalize from seen to unseen data. Nevertheless, in most benchmark datasets, while the images to segment vary, the annotation is often done by a single annotator. Therefore, it is not unlikely that it is the annotator's subjective outlook or bias that actually shapes the segmentation model and consequently influences the resulting image labels.

While the issue of inter-rater bias has significant implications, in particular nowadays, when an increasing number of deep learning systems are utilized for the analysis of clinical data [10, 15], it often seems to be neglected. In [1] deep learning is used to analyze the effect of common label fusion techniques on the estimate of segmentation uncertainty among observers. Nevertheless, the problem addressed there is completely different and the distinction between random versus consistent (i.e., bias) inter-observer variability is not made. Consistent differences in medical imaging data have been addressed for a related problem of inter-site variability by [16] for structural MRI and by [11] for diffusion MRI. In addition, inter-site variability was also investigated in the context of deep-learning in [5]. Yet, inter-site variability refers mainly to the differences in imaging data acquired by different machines and not the raters.

The main objective of this work is to quantify the impact of the observer's conception and competence on segmentation predictions by a supervised deep learning framework. In a sequence of experiments, utilizing both classifier- and segmenter-DNNs, we show that inter-rater bias affects significantly the DNN training process, and therefore leads to different segmentation results for the same test data, despite carefully using an identical DNN architecture and training regime. In fact, consistently lower Dice scores are calculated if training and

test segmentations are of different raters. We support our findings by training a classifier DNN to distinguish between different raters based on their segmentations. Surprisingly, much more significant rater-classification results were obtained when the segmentation predictions (the outputs of the segmentation DNNs) rather than the manual annotations (used for training) were considered. We then suggest a compromise training regime, that incorporates the segmentations of both raters.

For the purpose of this study, we used two different datasets. This includes a multi-modal MRI dataset of Multiple Sclerosis (MS) patients, that was made publicly available by the ISBI 2015 MS-lesion challenge [2] and a CT dataset of Intracerebral Hemorrhage (ICH) patients from a private source [8]. Each scan in both datasets is provided with annotations from two sources. The MS-lesion scans were annotated by two raters with different levels of expertise and the ICH scans were annotated manually and in a semi-automatic (semi-manual) manner with an interactive segmentation tool [8]. The interactive tool is based on proposal segmentation generated automatically, following its correction based on mouse clicks provided by the user. The results obtained allow us to highlight a worrisome clinical implication of DNN bias induced by inter-rater bias during training. Specifically, relative underestimation of the MS-lesion load by the less experienced rater was amplified and became consistent when the volume calculations were based on the segmentation predictions of the DNN that was trained on this rater’s input. In the same manner, the differences in ICH volumes calculated based on outputs of identical DNNs, each trained on annotations from a different source were more consistent and larger than the differences between the ICH volumes as calculated based on the manual and semi-manual annotations used for training.

The rest of the paper is organized as follows. In Section 2 we describe the data; the segmenter and classifier DNNs as well as the evaluation measures we used. In Section 3 we present the experimental results. We conclude in Section 4.

## 2 Methods

### 2.1 Data

**Multiple sclerosis (MS) Lesion MRI scans:** The multi-modal brain MRI dataset consists of 21 scans of MS lesion patients from the ISBI 2015 MS segmentation challenge dataset [2]. Scans were acquired by a 3T Philips scanner and include T1-w, T2-w, PD-w and FLAIR sequences. MS-lesions were annotated by two different raters with four (source #1) and ten (source #2) years of experience in delineating lesions. The second rater has overall 17 years of experience in structural MRI analysis. More details can be found in [2]. Fig. 1 presents two MRI slices along with the labels of both raters from the MS-lesion dataset.

**Intracerebral Hemorrhage (ICH) CT scans:** The brain CT dataset includes scans of 28 ICH patients acquired at the Soroka Medical Center with

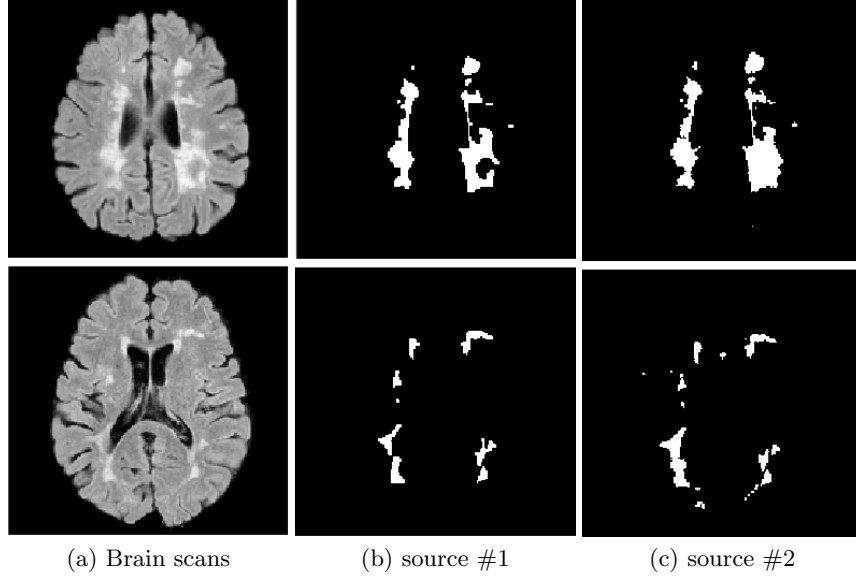


**Fig. 1.** MRI brain scans of MS patients annotated by two different raters. (a) 2D slices of 3D brain scans (FLAIR) (b-c) MS annotations of rater #1 and rater #2, respectively.

Philips Brilliance CT 64 system without radiocontrast agents injection. The size of each scans is  $512 \times 512 \times [90 - 100]$  voxels with voxel size of  $0.4 \times 0.48 \times 3$  mm<sup>3</sup>, with 1.5 mm overlap in the axial direction. Each scan was annotated by an experienced radiologist - manually (source #1) and with the help of a semi-manual segmentation tool (source #2) [8]. Fig. 2 presents a CT slice from the ICH dataset along with the manual and the semi-manual segmentations.

**Data patches:** Due to GPU memory limitations, we partitioned the data into overlapping patches. The ICH dataset was partitioned into cubic patches of size  $100 \times 100 \times 100$  voxels and the multi-modal MS-lesion data was partitioned to 4D patches of size  $100 \times 100 \times 100 \times 4$  voxels.

## 2.2 Neural Networks: Architectures and Training

The architectures of both the 3D U-Net - used for segmentation and the classifier CNN - used for rater identification, are illustrated in Figure 3.

**3D U-Net.** The U-Net is a symmetrical fully convolutional DNN with skip connections between its down-sampling and up-sampling paths [14]. For this study, we implemented a 3D U-Net [3] with Tensorflow and trained it for the MS-lesion segmentation of multi-modal 3D brain MRI scans (dataset #1), and for the ICH segmentation of 3D brain CT scans (dataset #2). For the MS-lesion dataset, we used a cross-validation scheme with 11, 5 and 5 brain scans for

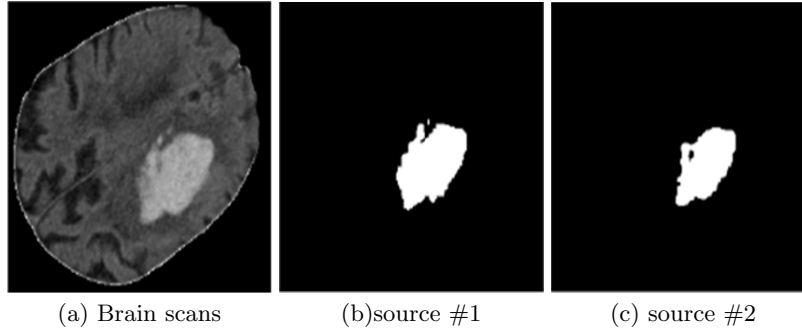


**Fig. 2.** A CT brain scan of an ICH patients with two different annotations. (a) A 2D slices of a 3D CT brain scan (b-c) ICH segmentations obtained by manual (source #1) and semi-manual (source #2) annotations.

training, validation, and testing, respectively, while for the ICH dataset we used a cross-validation scheme with 16, 4 and 8 brain scans for training, validation and testing, respectively. In both cases, training was based on the cross-entropy loss. As we mentioned before, due to GPU memory limitations, we used patches. As in the original U-Net paper [14], we favored large input patches over a large batch size and hence set the batch size to two with a learning rate of 0.0005. We also used batch normalization and dropout of 0.5.

**CNN Classifier.** The CNN classifier is used for rater identification based on either the actual annotations provided by the raters or based on the automatic segmentations provided by the U-Nets, where each network was trained on the annotations provided by either of the raters. The classifier’s architecture consists of 4 consecutive blocks, followed by a dense layer and a fully connected layer. Each block is comprised of 2 convolutions followed by one max pooling (besides the last one). We trained and tested the CNN classifiers based on volumetric ( $100 \times 100 \times 100$ ) patches extracted from the MS-lesion (21 brain scans) and the ICH (28 brain scans) datasets. Specifically, for the MS-lesion dataset, we used 7000 patches (11 brain scans) for training, 2800 patches for validation, and 2500 patches (5 brain scans) for the test phase. For the ICH dataset, we used 6914 patches (16 brain scans) for training, 2500 patches for validation, and 2600 patches (6 brain scans) for the test phase. As the sizes of the data sets were relatively small we ran these experiments with 2-fold cross validation, switching between the training, the test, and the validation sets. In addition, we ran each experiment multiple times. We used the cross entropy loss, a batch size of only 1, dropout of 0.5, batch normalization and set the learning rate to 0.001.

### 2.3 Quantitative evaluation measure

We use the Dice score [4] to quantify the compatibility between the manual segmentations of the two raters and to compare between the raters’ annotations and the segmentations generated by two 3D U-Nets, where each was exclusively

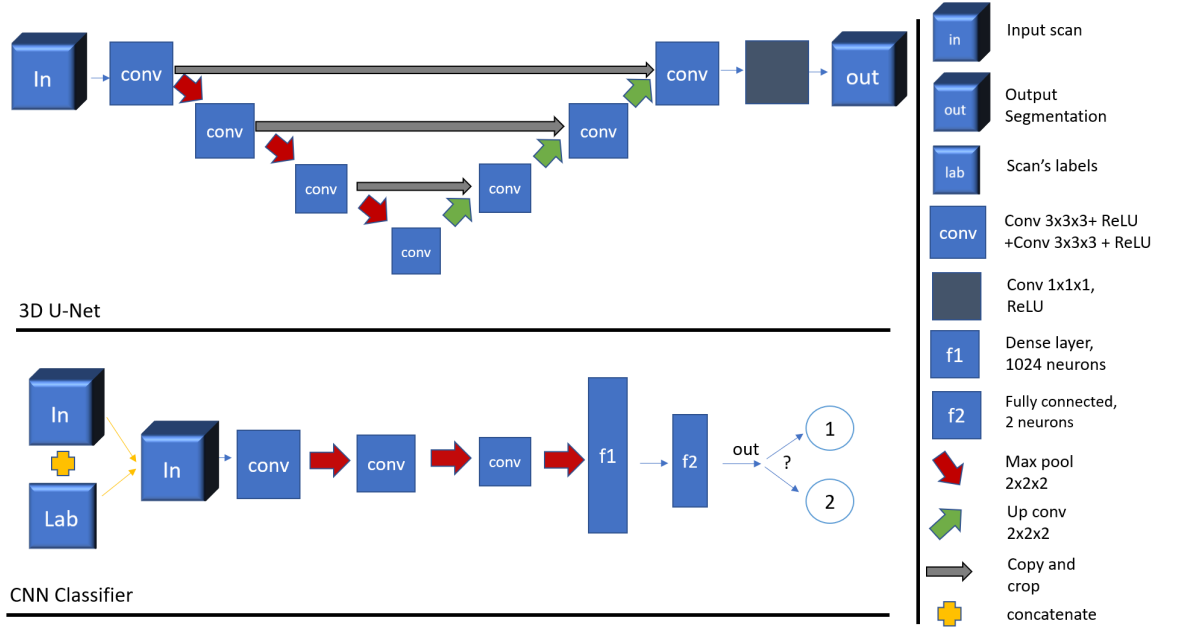


**Fig. 3.** DNNs architectures: upper panel: 3D U-Net for MS-lesion and brain ICH segmentation; lower panel: Classifier DNN for classifying the source of the segmentations

trained on the manual segmentations of either of them. We also present the accuracy of the classifier-CNN defined as the number of correctly classified segmentation patches per-brain (source #1 or source #2) with respect to the total number of patches.

### 3 Experiments

To assure that the results obtained are not affected by the random initialization of the network's weights, we trained the U-Net for each dataset and annotation source several times. Segmentation and classification results presented in the paper were obtained by averaging the DNNs' outputs.

#### 3.1 MS-lesion and Intracerebral Hemorrhage (ICH) segmentation for cross-evaluation

The mean Dice score between the manual segmentations of source #1 and the corresponding manual segmentations of source #2 is  $0.7341 \pm 0.0967$  for the MS-lesion dataset, and  $0.83 \pm 0.05$  for the ICH dataset, indicating significant mismatches between the sources. These mismatches can be visually observed in

Figs. 1-2. To demonstrate the impact of the different raters’ segmentations on the DNN training, we trained a 3D U-Net twice, each time with the segmentations of either of the raters. For the sake of convenience, we term the U-Nets trained on the segmentations of source #1 and source #2 by network #1 and network #2, respectively, although the very same architecture and training regime were used. We then tested the U-Net performances by comparing the manual segmentations of each of the raters with the output segmentations obtained for each of the training sessions. Thus, for each dataset, we performed four comparisons, either training and testing using the same source segmentations or training on one source and testing on the other (cross rater evaluation).

**Results:**

Figure 4 presents slices of 3D MRI scans from the MS lesion dataset (rows 1-2) and of CT scans from the ICH dataset (rows 3-4) along with the segmentations provided by two different sources (source #1 and source #2, columns 1-2) as well as the segmentations provided by DNNs (network #1 and network #2) each is trained on segmentations from a different source (columns 3-4). Note the relative visual similarity between the manual segmentations of source #1 (#2) and the DNN segmentations of network #1 (#2). Cross-evaluation Dice scores obtained by training based on source #1 and testing based on source #2 and vice versa are presented in rows 1-2 of Table 1 and Table 2 for the MRI and CT datasets, respectively. For comparison, the Dice scores obtained for training and testing with segmentations provided by the same rater are presented as well. Two-sample t-tests with p-values of  $9.9029e - 04$  for the MRI and 0.0167 for the CT datasets, indicate statistically significant differences between the Dice scores obtained for same-source experiments (in which segmentations of the same rater were used for both training and test) and cross-source experiments (in which the networks trained on the segmentations of one rater were tested on the segmentations of the other rater).

### 3.2 Mixed Source Training

**Experimental design.** In this experiment, we aimed to simulate a situation in which the number of training annotations provided by an expert is much smaller than the number of annotations provided by a less experienced annotator. We, therefore, trained a 3D U-Net multiple times with a mixed training set, containing a different number of annotations of the two raters. We then used the test sets to check the dependency between the Dice scores, calculated with respect to annotations provided by one of the sources, and the number of training annotations of that source.

**Results:**

For both the ICH and the MS datasets, we used the entire datasets provided by source #1 and only part of the annotations provided by source #2. The results, for the MS dataset, are presented in rows 3-5 of Table 1. The main finding is that the average Dice score, with respect to source #2 decreases from 0.8 (when the U-Net is exclusively trained on input from source #2) to 0.78 when the U-Net is

trained on input from source #1 and only one third of the input from source #2. Similar findings are obtained for the ICH dataset, as presented in rows 3-6 of Table 2. Here, the average Dice score, with respect to source #2 decreases from 0.86 (when the U-Net is exclusively trained on input from source #2) to 0.84 when the U-Net is trained on input from source #1 and less than one third of the input from source #2.

### 3.3 MS-lesion load and ICH volume

An important clinical measure is the MS lesion load which indicates the severity of the disease and may predict long-term cognitive dysfunction in MS patients [12]. The lesion load is estimated by the sum of voxels labeled as lesion. Figure 5 presents a bar plot of the lesion loads of 21 brain MR volumes as calculated from the segmentations of the raters and the networks. For clarity, brain indices (x-axis) were arranged in an increasing order of the estimated MS-lesion load. The plot shows that the lesion loads calculated from the manual segmentations from source #1 (yellow) are, for most brains (all of them but 6, circled in red/black), lower than the lesion loads calculated from the manual segmentations provided by source #2 (red). However, the alerting results refer to the network segmentations. MS-load estimations based on network #1 (black) segmentations are almost consistently (all of the brains but 1, circled in black) much smaller than the load estimations of network #2 (light blue), showing that inter-rater bias induces an increased and generalized bias between the networks.

Another important clinical measure is the ICH volume, which is a key factor experts take under consideration for deciding whether a patient needs to undergo a surgery or not. The load is estimated by the sum of voxels labeled as lesion. Figure 6 presents a bar plot of hemorrhage volume of 28 brain CT volumes as calculated from the segmentations of the raters and the networks. The plot shows that the ICH volumes calculated from the segmentations from source #1 (yellow) are, for most brains (all of them but 1, circled in red), higher than the ICH volumes calculated from source #2 (red). The figure also shows that when calculated by the networks, the hemorrhage volume is consistently (28/28) higher according to network #1(black), which corresponds with the results obtained in the MS-load experiment.

**Table 1.** MRI dataset: Dice scores of cross evaluation; same-rater and multi-rater

Trained/Evaluated	rater 1	rater 2
rater 1	$0.82 \pm 0.05$	$0.74 \pm 0.08$
rater 2	$0.72 \pm 0.10$	$0.82 \pm 0.07$
raters2+1 (ratio 11/11)	$0.8 \pm 0.08$	$0.79 \pm 0.09$
raters2+1 (ratio 05/11)	$0.79 \pm 0.06$	$0.77 \pm 0.06$
raters2+1 (ratio 04/11)	$0.78 \pm 0.05$	$0.77 \pm 0.04$



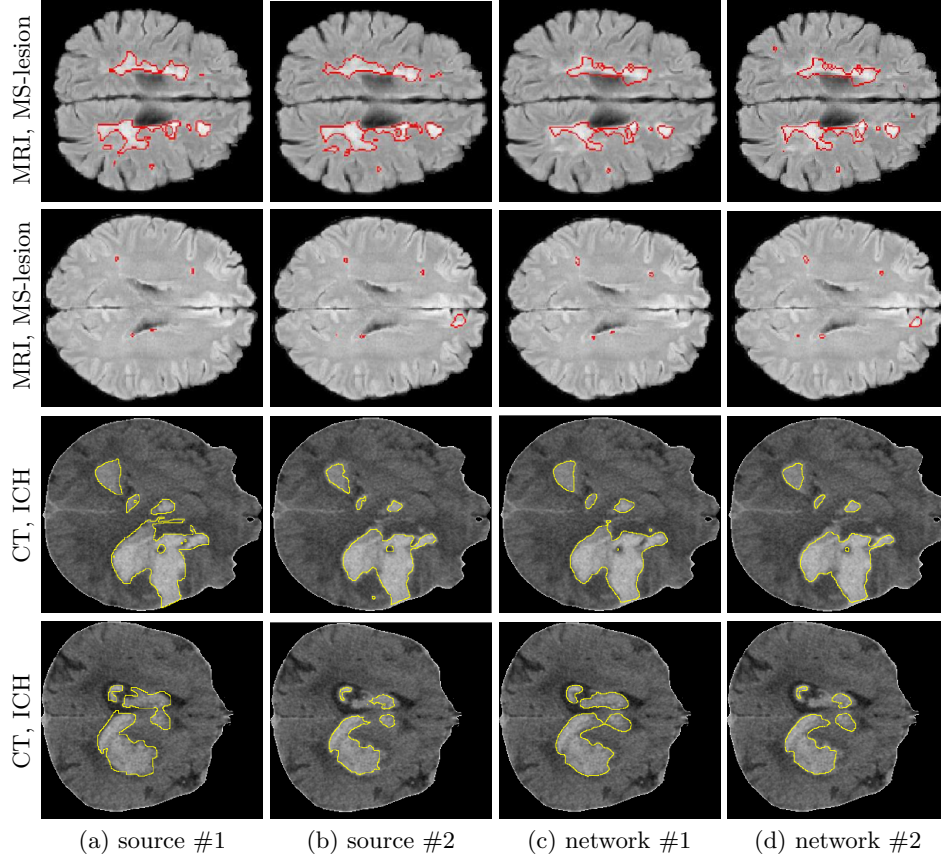


**Fig. 4.** MRI and CT scans of MS-Lesion and ICH patients, respectively, along with the manual (or semi-manual) and the U-Net segmentation contours. (a) Segmentations provided by source #1 (b) Segmentations provided by source #2 (c) Automatic segmentations of the U-Net, trained with the data labeled by the source #1 (d) Automatic segmentations of the U-Net trained with the data labeled by source #2.

### 3.4 Rater and network classification

**Experimental design.** To support our finding, we trained classifier DNNs to differentiate between the different segmentation sources based on the actual annotations. The input to each of the classifiers include pairs of images (CT or MRI) and the corresponding segmentations, randomly selected from either of the sources. The classifier was also used to distinguish between segmentation predictions of network #1 and network #2 which were trained based on the segmentations of source #1 and source #2, respectively.

#### Results:

The first row in Table 3 (MS-lesion data) and in Table 4 (ICH data) presents source classification results based on the respective manual annotations. The

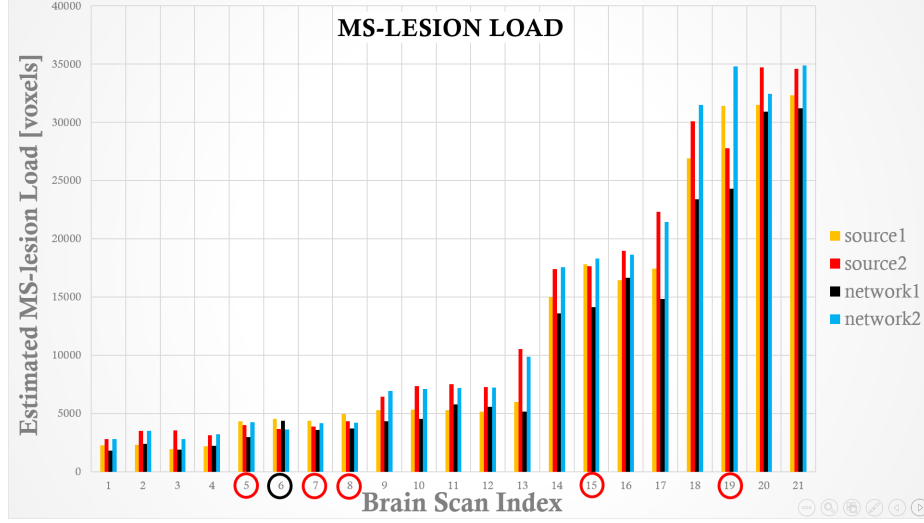


**Fig. 5.** Comparison of MS-lesion load estimate

successful classifications (hit rates of 0.87 and 0.917, respectively) indicate consistent differences between the segmentations provided by the different sources. The second row in each of the tables presents much better classification results (hit rates of 0.9 and 0.95, respectively) when the classifier CNNs are tested on segmentation predictions provided by the U-Nets (network #1 and network #2), rather than the source segmentations themselves. This implies that not only do the segmentations provided by each source have particular characteristics that can be distinguished by a classifier CNN, but also these distinguishing characteristics seem to be enhanced (or become more consistent) in the automatic segmentations of network #1 and network #2.

**Table 2.** CT dataset: Dice scores of cross evaluation; same-rater and multi-rater

Trained/Evaluated	source #1	source # 2
source # 1	$0.86 \pm 0.1$	$0.79 \pm 0.07$
source # 2	$0.80 \pm 0.09$	$0.87 \pm 0.07$
sources 1+2 (ratio 16/16)	$0.86 \pm 0.07$	$0.82 \pm 0.05$
sources 1+2 (ratio 8/16)	$0.84 \pm 0.07$	$0.81 \pm 0.06$
sources 1+2 (ratio 06/16)	$0.83 \pm 0.06$	$0.81 \pm 0.06$
sources 1+2 (ratio 05/16)	$0.82 \pm 0.10$	$0.80 \pm 0.07$

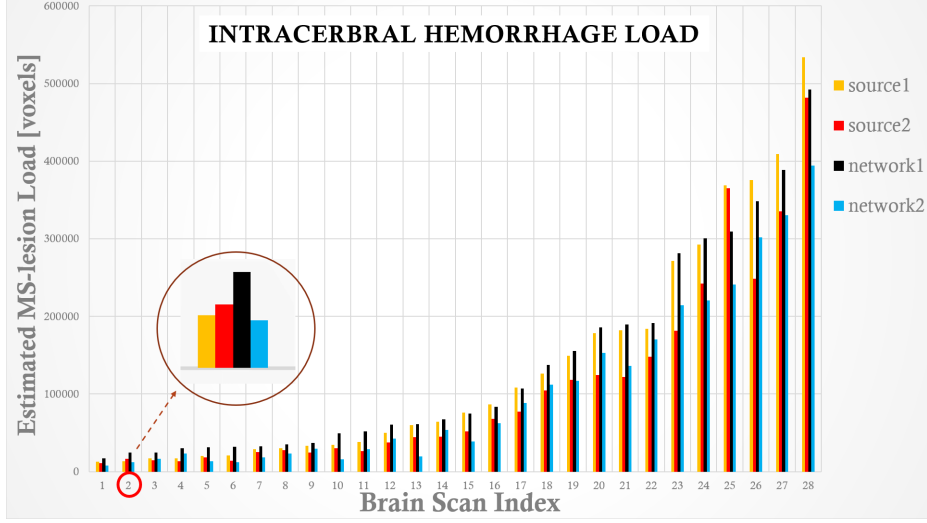


**Fig. 6.** Comparison of ICH load estimate

**Table 3. Classification results for MS dataset.** Mean classification hit-rates ( $\pm$  std) obtained by the classifier CNN for distinguishing between segmentations provided by the two sources (first row) and by the two U-Nets, where each was trained on either of the sources (second row).

	# of patches	classification hit-rate $\pm$ std
source #1 vs. #2	8441	$0.90 \pm 0.05$
network #1 vs. #2	8597	$0.93 \pm 0.03$

**Table 4. Classification results for the ICH data.** each classification hit-rates ( $\pm$  std) obtained by the classifier CNN for distinguishing between segmentations provided by the two sources (first row) and by the two U-Nets, where each was trained on either of the sources (second row).

	# of patches	classification hit-rate $\pm$ std
source #1 vs. #2	9260	$0.917 \pm 0.06$
network #1 vs. #2	9494	$0.95 \pm 0.04$

## 4 Conclusions and Discussion

In this paper, we highlighted the problem of inter-rater bias in medical image segmentation, which is often overlooked in the context of deep learning methods. Specifically, we exemplified the phenomenon of training-induced bias using CT and MRI datasets of ICH and MS-lesion patients scans (respectively) where each of these datasets was annotated by two different sources. While one could expect that DNNs trained with different target segmentations would converge in a different manner thus providing different test results, the amplification of

the differences between the DNNs' outputs was surprising. These findings are worrisome. MS-lesion loads are used for evaluating MS disease progress. Patient's ICH volume estimates are critical to the determination of the therapy procedure, which may involve surgery in addition to medicine intake. While the results shown are dataset-specific we believe that the phenomena of *DNN induced bias* is a general one, and as such has clinical implications that the biomedical imaging community should be aware of. Nowadays, when much effort is made to improve DNNs performances, the clinical training of the human annotator or the accuracy of the annotating source, that provided the 'ground truth' segmentations to the network, should be also considered.

Our study demonstrates that the expertise of the annotator directly influences DNN's training and consequently its test results. Since expert's annotations are costly and often only partially available we suggest a mixed training process, using annotations provided by two or more sources. Addressing the common situation in which a less experienced rater provides most of the annotated data, we show that it is sufficient to use a small portion of expert's annotations during training to influence DNN's performances.

## References

1. Alain, J., Raphael, M., Ekin, E., et al.: On the effect of inter-observer variability for a reliable estimation of uncertainty of medical image segmentation. In: MICCAI. pp. 682–690 (2018)
2. Carass, A., Roy, S., Jog, A., et al.: Longitudinal multiple sclerosis lesion segmentation: resource and challenge. *NeuroImage* **148**, 77–102 (2017)
3. Çiçek, O., Abdulkadir, A., Lienkamp, S., et al.: 3D U-Net: learning dense volumetric segmentation from sparse annotation. In: MICCAI. pp. 424–432 (2016)
4. Dice, L.R.: Measures of the amount of ecologic association between species. *Ecology* **26**(3), 297–302 (1945)
5. Gibson, E., Hu, Y., Ghavami, N., et al.: Inter-site variability in prostate segmentation accuracy using deep learning. In: MICCAI. pp. 506–514. Springer (2018)
6. Gordon, S., Lotenberg, S., Long, R., et al.: Evaluation of uterine cervix segmentations using ground truth from multiple experts. *Computerized Medical Imaging and Graphics* **33**(3), 205–216 (2009)
7. Hayward, R., Patronas, N., et al.: Inter-observer variability in the measurement of diffuse intrinsic pontine gliomas. *J. of Neuro-Oncology* **90**(1), 5761 (2008)
8. Hershkovich, T., Shalmon, T., Shitrit, O., Halay, N., Menze, B.H., Dolgopyat, I., Kahn, I., Shelef, I., Riklin Raviv, T.: Probabilistic model for 3D interactive segmentation. *Computer Vision and Image Understanding* **151**, 47–60 (2016)
9. Joskowicz, L., Cohen, D., Caplan, N., Sosna, J.: Inter-observer variability of manual contour delineation of structures in CT. *Eur Radiol.* **29**(3), 1391–1399 (2019)
10. Litjens, G., Kooi, T., Bejnordi, B., et al.: A survey on deep learning in medical image analysis. *Medical Image Analysis* **42**, 60–88 (2017)
11. Mirzaalian, H., De Pierrefeu, A., Savadjiev, P., et al.: Harmonizing diffusion MRI data across multiple sites and scanners. In: MICCAI. pp. 12–19 (2015)
12. Patti, F., De Stefano, M., Lavorgna, L., Messina, S.: Lesion load may predict long-term cognitive dysfunction in multiple sclerosis patients. *PLoS One* **10**(3) (2015)

13. Popovic, Z., Thomas, J.: Assessing observer variability: a user guide. *Cardiovasc Diagn Ther* **7**(3), 317–324 (2017)
14. Ronneberger, O., Fischer, P., Brox, T.: U-Net: Convolutional networks for biomedical image segmentation. In: *MICCAI*. pp. 234–241 (2015)
15. Shen, D., Wu, G., Suk, H.: Deep learning in medical image analysis. *Annu. Rev. Biomed. Eng.* **19**, 221–248 (2017)
16. Styner, M. and Charles, H., Park, J., Gerig, G.: Multisite validation of image analysis methods: assessing intra- and intersite variability. In: *SPIE Medical Imaging*. vol. 4684, pp. 278–286 (2002)
17. Warfield, S.K., Zou, K., Wells, W.: Simultaneous truth and performance level estimation (STAPLE): an algorithm for the validation of image segmentation. *IEEE transactions on medical imaging* **23**(7), 903–921 (2004)